Stabilization of Viruses by Encapsulation in Silk Proteins

Tara D. Sutherland,*,[†] Alagacone Sriskantha,[†] Jeffrey S. Church,[‡] Tanja Strive,[†] Holly E. Trueman,[†] and Tsunenori Kameda[§]

[†]Ecosystem Sciences, Commonwealth Scientific and Industrial Research Organisation (CSIRO), Clunies Ross Street, Acton, Australian Capital Territory 2601, Australia

[‡]Materials Science and Engineering, Commonwealth Scientific and Industrial Research Organisation (CSIRO), P.O. Box 21, Belmont, Victoria 3216, Australia

[§]National Institute of Agrobiological Sciences, 1-2 Owashi, Tsukuba, Ibaraki 305-8634, Japan

ⓢ *Supporting Information*

ABSTRACT: Viruses are important for a range of modern day applications. However, their utility is limited by their susceptibility to temperature degradation. In this study, we report a simple system to compare the ability of different dried protein films to stabilize viruses against exposure to elevated temperatures. Films from each of three different silks, silkworm, honeybee silk and hornet silk, stabilized entrapped viruses at 37 °C better than films of albumin from bovine serum (BSA) and all four proteins provided substantially more stabilization than no protein controls. A comparison of the molecular

structure of the silks and BSA films showed no correlation between the ability of the proteins to stabilize the virus and the secondary structure of the protein in the films. The mechanism of stabilization is discussed and a hypothesis is suggested to explain the superior performance of the silk proteins.

KEYWORDS: *bacteriophage, coiled coil, vaccine stabilization, biocontrol, FTIR, protein stability*
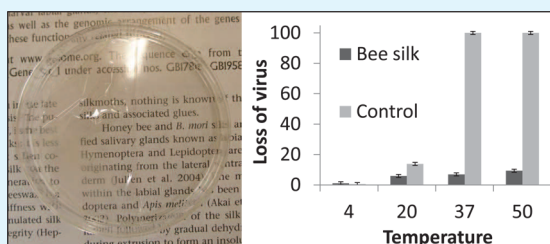
■ INTRODUCTION

Although commonly associated with pathology, viruses fulfill many beneficial roles in the modern world: attenuated or inactivated viruses provide health benefits to humans and livestock as vaccines, and virulent viruses are used in pest control.[1] Furthermore, genetically modified viruses are playing a growing role as vehicles to fight cancer or for gene therapy, with many hundreds of trials already completed or underway, and as agents to specifically treat pathogenic bacteria.[1]

However, many viruses are susceptible to temperature inactivation. Exposure to ambient temperatures can quickly reduce their survival rates or structural integrity. They therefore need to be transported and stored with refrigeration. This compromises their use for human vaccines, especially in the developing world, and has led to the establishment of an extensive network of refrigeration, "the cold chain", to enable their distribution. The cold chain is expensive and prone to sporadic failures. Veterinary vaccines and virulent viruses used in agriculture are also frequently compromised by temperature effects. For example, in Australia, rabbit hemorrhagic disease virus (RHDV) has been used since 1996 to control feral rabbits, a serious environmental and economic pest.[2] Vials of frozen RHDV can be purchased to control rabbits, but the infectivity of the virus declines quickly if stored incorrectly, often because land managers either lack the resources or the training of medical or veterinary personnel.

In an effort to develop vaccine formulations to protect against failures in the cold chain, the Kaplan laboratory investigated stabilization of the live measles, mumps and rubella (MMR) vaccine within water-soluble silkworm silk protein matrices prepared from dissolved natural silk cocoons.[3] A high proportion of the viruses encapsulated within the silk remained viable for up to 25 weeks at elevated temperatures (up to 45 °C). Virus infectivity is mediated through the virus coat proteins. In the absence of silk matrices, viral inactivation at elevated temperatures is most commonly due to localized unfolding of the viral surface proteins.[4] It was proposed that the silk protected the virus at least in part by replacing or stabilizing the water hydration shell surrounding the virus and that this protected the surface of the virus, both physically and chemically. Supporting this, the authors used differential scanning calorimetry (DSC) to demonstrate a 51.5 °C increase in a thermal transition observed when heating the virus in water compared to heating the virus entrapped within the silk.[3] Even in solution, the silk played a role in preventing viral protein conformational changes and concurrent viral aggregation at 16.8 °C, although it was not determined whether this was sufficient to stabilize the virus against exposure to elevated temperatures. Increasing the viral glass transition temperature (T_g) and prevention of aggregation was proposed to account for the stabilization of LaSota virus by the nonprotein polymers polyethylene glycol and dextran.[5]

ACS Publications © 2014 American Chemical Society

18189

dx.doi.org/10.1021/am5051873 | *ACS Appl. Mater. Interfaces* 2014, 6, 18189−18196

Here, we have tested whether other silks can also stabilize viruses. "Silk" is a functional definition that refers to fibrous protein materials produced by arthropods from concentrated protein solutions accumulated in dedicated silk glands[6] and as such, not all silks have the same architecture or molecular structure. Natural silkworm silk is made from large proteins with highly repetitive amino acid sequences that adopt primarily a β-sheet structure.[7] In contrast, the silk proteins of honeybees and hornets are small and nonrepetitive. Native honeybee silk contains high levels (around 65%) of α-helices and low levels of β-sheets (around 10%)[8] whereas the homologous native hornet silk has similar α-helical regions with somewhat more extended β-sheet regions.[9,10]

Viruses such as the live viruses in the MMR vaccine used by Zhang et al.[3] represent some of the most temperature and environmentally sensitive viruses (for example, see ref 11) but assessing viral viability can be difficult. Zhang et al.[3] used an assay for virus infectivity based on quantitative real-time reverse transcriptase PCR (qPCR), in which cultured mammalian cells were exposed to solutions of dissolved silk-entrapped virus films. The cells were allowed to replicate for 3 days, then the amount of viral RNA present in the infected cells was determined by qPCR. The method is time-consuming and technically demanding. So, in order to compare viral survival rates across multiple silk types and different temperatures, we developed an assay using a bacteriophage as a model virus. Bacteriophages had been suggested previously as a model system to study environmental stability of nonenveloped viruses.[12] They offer the advantages of being commercially available and being easy to work with. In general, they are relatively stable at low temperatures, but susceptible to inactivation at ambient and higher temperatures. Systems that directly assess phage infectivity are suitable as models for the stability of both live and inactivated/subunit vaccines because the preservation of the three-dimensional and antigenic structures is a prerequisite for either type to work effectively.[13]

Veterinary vaccines are often based on live attenuated or inactivated nonenveloped viruses, including vaccines for the feline calicivirus and panleukopenia virus,[14] canine distemper, hepatitis and parvovirus,[15−17] foot and mouth disease[18,19] and rabbit hemorrhagic disease virus.[20] Inactivated or subunit human vaccines include hepatitis A[21] and human papillomavirus vaccines.[22] Live attenuated human vaccines include the rotavirus vaccine[23] and a type of polio vaccine (Sabin, Oral Polio Virus (OPV), although the OPV vaccine has been discontinued in many countries and is either replaced by or used in combination with an inactivated polio vaccine (IPV).[24] Bacteriophages themselves are being developed as highly specific antibacterial agents for control of some pathogenic bacteria (see refs within[25,26]). Here we describe a bacteriophage system to assess and compare the ability of different silks to stabilize viruses against exposure to elevated temperatures.

■ EXPERIMENTAL SECTION

Preparation of Silk Protein Solutions. Honeybee silks: The honeybee silk gene (AmelF3; accession number AC149702) was amplified using oligonucleotide primers GGA ATT CCA TAT GGG CGT CGA GGA ATT CAA GTC CTCG and CGG CAG ATC TTT ATT AAA ATT TTT TAT CCT CAA TA (restriction enzyme sites NdeI and BglII underlined) and the amplicon was cloned into the NdeI and BglII sitesof the pET14b vector (Novagen) to generate a 6xHis tagged construct. Expression vectors were transformed into Rosetta 2 (DE3) cells (Novagen) and grown on Luria−Bertani (LB) broth ampicillin (Amp) plates overnight at 37 °C. Single colonies were

used to inoculate 25 mL of LB broth with 100 $\mu g \cdot mL^{-1}$ Amp then left to grow at 37 °C for 4 h. The starter culture was added to 1 L of Overnight Express Instant TB medium (Novagen) with glycerol (10 mL·L^{-1}) and 100 $\mu g \cdot mL^{-1}$ Amp, and grown overnight at 37 °C. The cells were spun down and the pellet resuspended in Bugbuster master mix (Novagen) and allowed to stand at room temperature for 1 h. The inclusion bodies were collected by centrifugation, washed with neat and then 1:10 dilution of the Bugbuster reagent then stored at −80 °C until required.

AmelF3 inclusion bodies were dissolved in 20 mL of phosphate buffer (GE Healthcare) containing 6 M guanidinium HCl (GuHCl) and 40 mM imidazole overnight at 4 °C and then filtered through a 0.22 μm filter (Millipore). The protein solution was loaded onto a HisTrap HP column (GE Health Care) that had been washed with 20 mL of phosphate buffer containing GuHCl and 40 mM imidazole, then washed with 20 mL of phosphate buffer containing GuHCl and 40 mM imidazole, then with 20 mL of phosphate buffer containing 40 mM imidazole and then the protein was eluted in phosphate buffer containing 250 mM imidazole. Fractions containing silk protein were identified after sodium dodecyl sulfate polyacrylamide gel electrophoresis (SDS-PAGE) chromatography on 4−12% NuPAGE Bis-Tris gels (Novagen) then transferred into a Slide-A-Lyser cassette with molecular weight cutoff of 10 000 (Thermo Scientific) and dialyzed against 100 mM NaCl overnight at 4 °C. The dialyzed material was concentrated by ultrafiltration (Vivaspin columns; Sartorius Stedim Biotech). The protein concentration was determined (BCA assay; Sigma) then the concentrated solution was dialyzed either against 100 mM NaCl or equal w/w glycerol overnight at 4 °C. The protein was stable under either of these conditions for at least 2 weeks. When required, the salt or glycerol was removed using a desalting column (Histrap Desalting column, GE Healthcare) according to the manufacturer's directions. The final concentration of the silk protein was determined from the mass remaining after drying a known volume of the solution.

Hornet silk: Hornet nests of *Vespa simillima xanthoptera* were collected from a field in the city of Tsukuba, Japan. Hornet cocoon silk (1.5 g) from the nests was dissolved in 30 mL of 9 M aqueous lithium bromide (LiBr; Wako Pure Chemical Industries, Japan) at 35 °C for 15 min. The LiBr solution of hornet silk was dialyzed against 0.1 N ammonia at 5 °C,[28] with the solution changed four times over a 24 h period. The final concentration of the silk protein, determined by thermogravimetric analysis (TGA) using Thermo plus TG8120 (Rigaku), was 2.5 wt %.

Silkworm silk: Aqueous solutions of silk fibroin (2.0 wt %) were obtained by dissolving degummed silk fibers from *Bombyx mori* in 9 M aqueous LiBr solution, followed by dialysis against deionized water.

Preparation of Protein/Virus Films. Virus (M13KO7 Helper Phage, order number N0315S, New England Biolabs) stock (10^{11} plaque forming units (pfu)·mL^{-1}) was diluted in filter sterilized TMS buffer (50 mM Tris−HCl, pH 7.5, 10 mM magnesium sulfate, 100 mM NaCl, 0.01% gelatin) to give 10^8 pfu·mL^{-1}. Proteins were prepared at 4.5 mg·mL^{-1} in distilled water. Virus was added to protein solutions to give 4×10^5 pfu in 200 μL of silk solution and then aliquots were placed into 5 mL Wheaton glass serum bottles (Aldrich, Z113964) and allowed to dry at room temperature. Albumin from bovine serum (BSA) was obtained from Sigma-Aldrich. Controls were prepared first with only virus without protein and second by substituting BSA for the silk protein. Vials containing dried protein and virus films or dried virus were placed in a vacuum desiccator for 12 h, sealed in a glovebox containing 95% nitrogen and 5% hydrogen, to remove trace oxygen (Wheaton closed top seals and stoppers; Aldrich, Z114146, Z114200) then placed at various incubation temperatures.

Assay of Virus Survival. A culture of *Escherichia coli* K12 ER2738 (New England Biolabs) was grown in 20 mL of Luria broth with 10 $\mu g \cdot mL^{-1}$ tetracycline overnight at 37 °C, and 2 mL of this culture was used to set up a 20 mL culture without tetracycline that was grown for 3−4 h. One milliliter of TMS buffer was added to vials to dissolve virus−silk films at 4 °C (honeybee silks and controls, 30 min; hornet and silkworm silks, overnight). The dissolved films were diluted to the desired pfu with TMS buffer and 100 μL mixed with 200 μL of the *E.*

coli K12 ER2738 cell culture then incubated for 20 min at 37 °C. Magnesium sulfate (50 uL of 1 M) and liquid top agarose at 45−48 °C (5 mL; 10 g tryptone, 5 g yeast extract, 5 g NaCl and 0.7 g agarose per liter) were added and the mixture poured into the top of warmed LB agar plates. The plates were incubated overnight at 37 °C to allow the *E. coli* to form a lawn and each virus to form a single plaque within that lawn. After incubation, the plaques were counted and numbers recorded. Plaques could be seen more clearly after 3−4 h of incubation at 4 °C.

Moisture Content and Rate of Dissolution of Films. Thermogravimetric analysis was conducted using a Thermo plus TG8120 (Rigaku) in a nitrogen flow (200 mL.min^{-1}), over the temperature range from room temperature to 180 °C at a heating rate of 10 °C.min^{-1}. Films were equilibrated to 25 or 37 °C at room temperature humidity (20%) prior to analysis. The rate of film dissolution was determined after approximately 2 mg of film was placed in 1 mL TMS buffer (see above). Samples were taken for up to 24 h and the amount of protein in solution was determined using the BCA assay (Sigma).

Film Secondary Structure Comparison. Infrared attenuated total reflectance (ATR) spectra were collected from the films using a PerkinElmer (Beaconsfield, UK) System 2000 Fourier transform infrared (FTIR) spectrometer fitted with single bounce ZnSe Pike Technologies MIRacle ATR accessory (Madison, USA) and a liquid nitrogen cooled mercury cadmium telluride detector. Spectra were collected at 4 cm^{-1} resolution with 64 scans coadded. Spectra obtained from several locations of each sample revealed little variability. All spectroscopic data manipulation was carried out using Grams AI V 9.1 software (Thermo Fisher Scientific, Waltham, USA). For comparison purposes, all infrared spectra were normalized on the amide I band at ~1643 cm^{-1}.

Secondary structure comparison was carried out by spectral deconvolution of the amide I region for all films and of the amide III region for the honeybee, hornet and BSA films. Spectral deconvolution was carried out by first identifying band components from the second derivative spectra obtained using the Savitzky−Golay method.[29] In fitting the zero order amide I region, a linear baseline defined by the intensity at 1733 cm^{-1} was utilized with additional peaks being fit well past the spectral region of interest in the low wavenumber side. For the amide III region the baseline was defined at 1193 cm^{-1} and additional peaks were added on the low wavenumber side. Fits were based on the usage of a minimal number of band components, each represented by a variable mixture of Gaussian and Lorentzian functions. All peak heights were limited to the range greater than or equal to zero. In the initial fitting steps the band centers were only allowed to vary by ±5 cm^{-1} from the frequency determined by the second derivative spectra. Component peaks with intensities less than 1.5% of the most intense component were deleted from the model. In the final refinements all parameters were allowed to vary unconstrained.

■ RESULTS

Development of Assay to Determine Virus Survival. We developed a simple method to determine survival of virus in silk protein matrixes (Figure 1). Cleared areas in *E. coli* lawns correspond to a single original infectious virus; therefore, the assay is a direct measure of virus viability. The assay allowed us to readily measure differences of 3 orders of magnitude in virus titer over the relevant time period. As with the assay described by Zhang et al.,[3] baseline survival rates were measured immediately after the initial film preparation. As we were interested in the stability of the virus during storage, no effort was made to optimize viral survival during film preparation. We monitored virus survival at different temperatures for up to 8 weeks (Figure 2). In the absence of protein, the virus showed no significant loss of infectivity after storage at 4 °C, significant loss at 20 °C, and at body temperature and higher, the virus rapidly lost all infectivity.
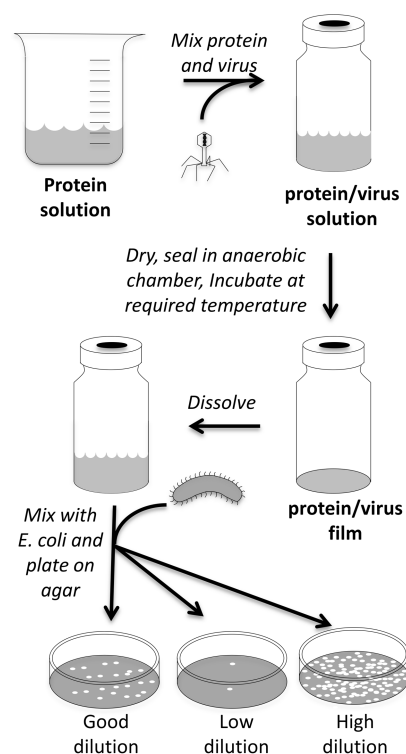

Figure 1. Schematic showing the method used to monitor virus survival in protein films at different temperatures. Virus is mixed with protein solutions, dried and incubated for the required time and temperature. Films with entrapped virus are then dissolved and aliquots are mixed with *E. coli* cells. The virus adsorbs onto bacterial cells, the virus/bacteria are mixed with warm agarose and then poured on top of prewarmed agar plates. Each original viable virus results in the formation of a "plaque", a circular area of lysed bacterial cells that can be easily visualized.
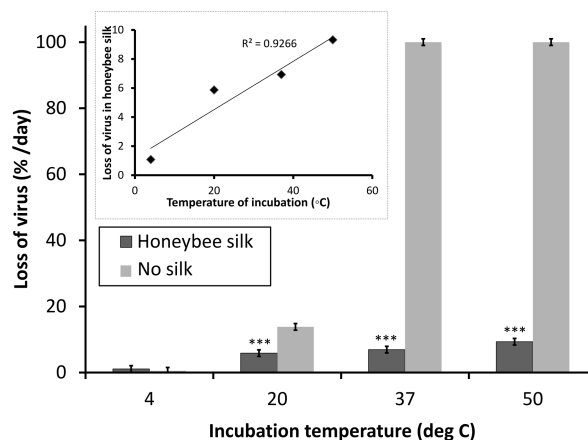
Figure 2. Loss of viral infectivity after incubation at various temperatures with and without honeybee silk protein. Inset shows linear relationship between incubation temperature and loss of virus. Error bars indicate standard errors. Asterisks (***) indicate that the loss of viable virus in the honeybee silk samples were different from corresponding controls without silk (2-tailed *t*-test, $p < 0.01$).

Relative Performance of Different Protein Films for Stabilization of Virus. We compared the ability of different silk films to stabilize virus stored at 37 °C for 8 weeks (Figure 3). BSA films were used for a nonsilk protein control. All proteins stabilized the virus at the elevated temperature.
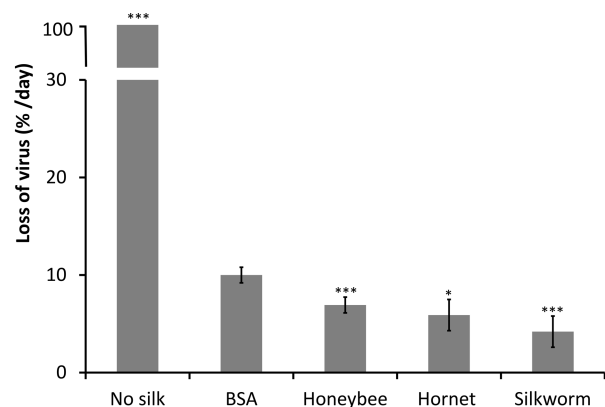
Figure 3. Loss of viral after incubation at 37 °C with and without various proteins. Error bars show standard errors. Less virus viability was lost from the silk containing films than from the BSA containing films (2-tailed *t*-test, *** *p* < 0.01, * *p* < 0.05).

Without protein, all viable virus was lost. Survival of the virus in the three different silks (94−96%) was greater than virus survival in the BSA containing samples (90%) (*p* < 0.05, 2-tailed *t* test).

Molecular Structure of Proteins. Native silks have excellent mechanical strength, flexibility and are generally insoluble in water in the absence of chaotropes, properties that are a consequence of their molecular structure: silkworm silk has high levels of β-sheets,[7] honeybee silk has high levels of α-helices,[8] and hornet silk has high levels of both α-helices and β-sheets.[9] However, recovery of live virus after entrapment in silk films requires that the silk protein matrixes can be dissolved in benign and biocompatible aqueous solutions. Consequently, any practical silk protein film used to stabilize viruses cannot be folded in its characteristic "water-insoluble" native state. Film casting conditions can dramatically affect silk protein folding and the proportion of α-helix, β-sheet and disordered structures (for example, see refs 27 and 30). Because of this variability in molecular structure as a function of casting conditions, we used FTIR to investigate correlations between the molecular structure of the proteins and their ability to stabilize viruses (Figure 4).

Comparison of the amide I and III regions of the spectra show that the molecular structures of the protein films differ.
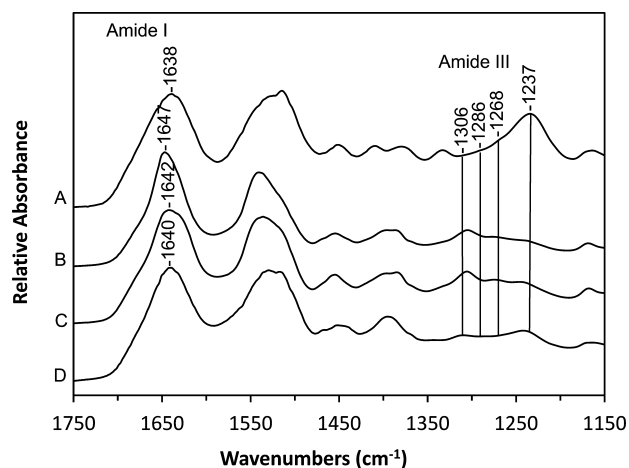
Figure 4. Infrared ATR spectra obtained from virus doped films: (A) silkworm, (B), honeybee, (C) hornet and (D) BSA.

The amide I peak maxima ranges from 1647 cm^{-1} for the honeybee protein film (Figure 4B) to 1638 cm^{-1} for the silkworm silk (Figure 4A). The coiled coil molecular component of the honeybee and hornet silks presents a particular issue in the analysis of the amide I region, with overlap of the five band components of this conformation[31−34] with band components associated with β-sheets, random coils and β-turns and bends.[29,30] In contrast, the band components in the amide III are much better resolved with band component groups near 1306, 1286, 1268 and 1237 cm^{-1} that have been associated with α-helical, β-turn and bend, disordered and β-sheet structures, respectively.[34−36] Details of the amide I deconvolutions for all of the films included in this study are presented in the Supporting Information (Figures S1−7). In addition, amide III deconvolutions are presented for the coiled coil silks and the BSA films. A summary of the distribution of the protein conformations of the various films based on the component peak areas of the amide I region is presented in Table 1.

Table 1. Protein Conformation Based on Analysis of Amide I Region[a]

film type	β-sheet (%)	α-helix (%)	β-turn (%)	random coil (%)
silkworm	25	18	25	32
honeybee	15	51	14	19
hornet	24	44	15	17
BSA	28	30	21	21

[a]Details of the deconvolutions are described in the Supporting Information.

Amide I band analysis of the silkworm protein film suggests a structure with 25% β-sheet, 18% α-helical, 25% β-turn and 32% random coil. This is in good agreement with previous results (23% α-helical, 22% β-sheet, 31% random coil and 24% β-turn) obtained using comparable experimental conditions by Tretinnikov and Tamada.[29] Those authors suggested that this conformation represents the bulk of the film, as when more surface sensitive ATR conditions are used the β-sheet component drops to 13%.

Conformational analysis of the amide I band of the spectrum obtained from the honeybee silk film indicates a structure with 51% α-helical (coiled coil), 15% β-sheet, 19% random coil and 14% β-turn, in good agreement with a previous estimate of 59% coiled coil.[8] In this earlier study, partially due to the complexity of the five coiled coil band components, the remaining structure was attributed to β-sheet content with no attempt being made to separate out random coils and β-turns. In this study, deconvolution of the amide III region (see the Supporting Information) suggests the structure is comprised of 48% α-helical (coiled coil), 12% β-sheet, 17% random coil and 23% β-turn, in reasonable agreement with the amide I analysis presented in Table 1, with the largest discrepancies being associated with coiled coil band component overlap with random coil and β-turn. The coiled coil band in the random coil band component that overlaps with the β-sheet components is the weakest and thus has the least effect.[33]

The protein conformational structure of the hornet silk film was similar to that of the honeybee but with less coiled coils and more β-sheets and turns (Table 1). The analysis of the amide III region (47% α-helical (coiled coil), 24% β-sheet, 9% random coil and 20% β-turn) supports the increase in β-sheet

structure. Similarly, native hornet silks are known to have higher β-sheet content then the native silk of bees.[37,38]

The band profile of the BSA in our films, 30% α-helical and 28% β-sheet, was similar to previously described data obtained from analysis of the amide I region of lyophilized solutions of BSA (31% α-helical and 30% β-sheet).[39] Deconvolution of the amide III region (see the Supporting Information) gave similar results: 29% α-helical, 26% β-sheet, 33% random coil and 12% β-turn. This structure is in good agreement with that obtained from BSA treated with 4 M guanidine hydrochloride[36] where deconvolution suggested a structure with 31% α-helical, 25% β-sheet, 32% random coil and 14% β-turn. Note that the discrepancy between the amide I and III band analysis is in the distribution of the more unordered protein structures. The structure is distinct from that of the crystallized form of BSA, which contains around 73% α-helices with the remainder being 3(10) helix, turns and coils.

Film Hydration and Dissolvability. One of the factors influencing virus survival in silk protein matrixes is hydration conditions.[3] We used two methods to compare the hydration conditions and solvent accessibility of the various films: TGA to determine residual water content and protein assays to determine the rate of film dissolution. TGA found that the residual water content of the silks and BSA equilibrated at 25 °C were similar (7.45 ± 0.35% honeybee silk films, 7.23 ± 0.05% hornet silk, 7.29 ± 1.45% silkworm silk films and 7.71 ± 0.11% for dried BSA). Greater differences were observed when films were equilibrated at 37 °C, with silkworm silk films being the driest (5.06 ± 0.35%), followed by BSA (6.27 ± 0.20%), honeybee silk (7.83 ± 0.23%) and the hornet silk had the greatest residual water content (7.92 ± 0.05%). Nonetheless, the BSA films dissolved immediately when placed in water (data not shown). The hornet and honeybee silk films absorbed water more rapidly than the silkworm silk and were completely dissolved within 30 min at 4 °C (Figure 5). The silkworm silk took more than 6 h to dissolve (Figure 5). TGA profiles are shown in Figure S8 (Supporting Information).

■ DISCUSSION

The model system described in this report is a direct assay of undamaged, functional, infectious bacteriophage viruses. Infectivity depends on the preservation of many protein structural features on the surface of a bacteriophage. Any treatment that preserves infectivity of a bacteriophage is also
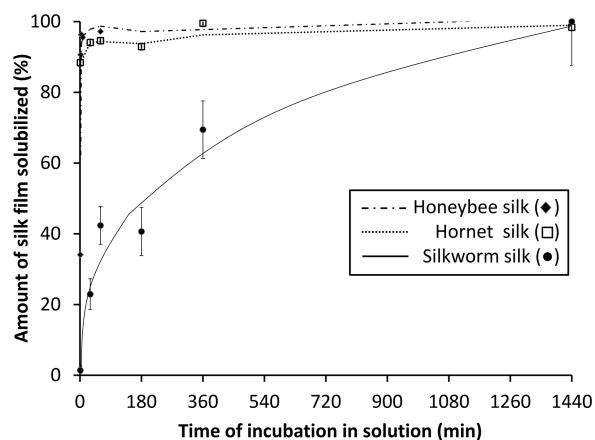
Figure 5. Comparative rate of dissolution of silk films. Bars indicate standard errors.

likely to preserve the structural integrity of any nonenveloped virus particle—a prerequisite for the effectiveness of vaccines based on live attenuated viruses, inactivated viruses, or virus-like particles (VLP).[13] We suggest that this system is a suitable model to assess the likely stability of all kinds of nonenveloped viruses under diverse environmental conditions.

Of the different types of proteins investigated here, silkworm silk was best able to stabilize the virus (virus loss of 4.2%/day at 37 °C), although the virus infectivity half-life at 37 °C ($t_{1/2}$ = 2.3 weeks) in our system was less than previously reported for lipid enveloped viruses in similar silk films (nonlyophilized films; $t_{1/2}$ = 22.0 weeks).[3] The honeybee and hornet silk proteins in our study were also able to stabilize virus and all silks were distinctly better at preserving virus infectivity than BSA. Nonetheless, BSA also conferred considerable stabilization against exposure to elevated temperatures relative to no added protein.

Enhanced thermal stability of viruses in artificial polymers and protein polymers has previously been associated with an increase in the glass transition temperature (T_g) of the virus coat proteins.[3,5] However, because the T_g is considerably greater than the temperatures under investigation here, it is likely that increasing the T_g is the result of stabilization rather than the cause. Stability has also been associated with protection against specific thermal degradation events: Zhang et al.[3] observed that the viral aggregation that occurred at 16.8 °C was delayed until 68.3 °C in the presence of solutions of silkworm silk. However, the increasing loss of virus with increasing temperature in our study was linear rather than discontinuous (inset, Figure 1) suggesting that no specific thermal events played an important role. Here we propose two mechanisms, drawn from the protein stability literature, which could explain why encapsulation within protein matrices protected the virus against temperature inactivation.

Infectivity of viruses requires specific interactions of the virus surface proteins with cell surface receptors, and denaturation of these viral surface proteins is associated with a loss of infectivity. The stability of the viral surface proteins can be expected to be influenced by internal factors such as interactions between the protein backbone and amino acid side chains, and side chain−side chain interactions, as well as external factors such as the hydration shell, the one to two layers of water molecules that surround the protein. In particular, fluctuations in the hydration shell underpin conformational changes on the surfaces of proteins.[41] It is likely that the protein-rich environment of the virus within protein matrices influences the hydration shell surrounding the virus. The hydration shell of proteins has a markedly higher density than that of bulk water.[42] Higher density water is slower to exchange and these reduced rates of exchange have the effect of reducing the rates of local protein unfolding.[43] In the protein matrices it is expected that the hydration layer will be influenced by both the viral surface proteins as well as the protein matrix and will have higher density, lower exchange rates and therefore less detrimental effect on protein structure than in the absence of the protein matrices. Therefore, a likely mechanism that enhances thermal stability of the viruses is the presence of high density water generated from the protein-rich environment within the protein matrixes.

A second factor that could protect the viral surface proteins against denaturation is hydrogen bonding between the protein matrices and the surface proteins of the virus. Protein−protein hydrogen bonds are shorter than water−protein hydrogen

18193

dx.doi.org/10.1021/am5051873 | ACS Appl. Mater. Interfaces 2014, 6, 18189−18196

bonds and therefore, in the presence of protein−protein hydrogen bonds, protein structures are more compact.[43] As proteins are compacted, molecular motion is constrained. Therefore, proteins in a compact state are more stable than those in a relaxed state,[44] less prone to partial unfolding,[45] and consequently more resistant to temperature denaturation. Interestingly, if the virus stabilizing mechanism does involve partially replacing the hydration shell surrounding the virus particle with hydrogen-bonding to the matrix protein, then it is likely that protein-based formulations will also prove advantageous in protecting viruses against freezing, a significant cause of damage to viruses during distribution.[4]

Both of the mechanisms described above depend on the hydration state of the protein: in the first, the proteins cause the hydration layer to become more ordered hence less mobile; in the second, the hydration layer is supplemented by protein−protein interactions. Both mechanisms may contribute to virus stabilization. This would be consistent with the observation of Zhang et al.,[3] that the best stabilization was observed with their driest silk preparation (1.9−2.2% water content) but silk preparations with 4.6−5.9% water content provided better stabilization than those with intermediate water content (2.5−3.9%). In our study, there was little variation in water content between the various films.

The two mechanisms described above would be expected to apply for any protein matrix and do not explain why the silk proteins offered superior protection to the virus at elevated temperatures over BSA. There was no correlation between protein size and its ability to stabilize the virus: silkworm silk protein is around 250 kDa, BSA is around 66 kDa and hornet and honeybee silks are 30−50 kDa. Silk proteins, in their native form, are known to pack together well. However, the proteins in the cast films do not contain silk proteins in their native secondary or tertiary structure, so it is unlikely that this explains the ability of the silk proteins to better stabilize the virus. There is also no obvious correlation between proportions of various secondary structures and the ability to stabilize the virus (Table 1). The best performing material (silkworm silk) and worst performing (BSA) are similar in having less order forming structures (α-helices and β-sheets) with 43% and 58%, respectively. There was also no correlation between the total number of charged residues or polar residues and the ability to stabilize the virus, with BSA having similar levels of polar residues to silkworm silk and similar levels of charged residues to hornet and honeybee silks. In the absence of any information about the atomic level structure of any of the proteins in the films, we were unable to look at correlations between the distribution and type of surface residues and stabilization. However, there is a correlation between the overall number of smaller residues (glycine, serine and alanine) of the four protein samples investigated in this study and the ability of films of that protein to stabilize the virus ($R^2 = 0.88$). It could be expected that the side chains of these smaller residues could pack more efficiently than larger side chains and that more dense packing would influence the hydration sphere. The side chains of alanine and glycine have low hydration potential[46] and hence protein matrices containing high levels of alanine and glycine residues are likely to drive water out of the hydration sphere and promote matrix protein to virus hydrogen bonding; serine has greater hydration potential,[46] implying that it will effectively pull water into the matrices. However, the small size of serine is expected to allow close packing of the proteins and therefore minimize the space available for bulk water. Serine is therefore

more likely to influence the hydration layer surrounding the virus. Consistent with this is the observation that the most stabilizing material (silkworm silk) has the highest proportion of alanine and glycine residues and took the longest time to redissolve whereas all the other materials dissolved rapidly. For virus stabilization, a trade-off may be required between maximizing dehydration to provide maximum stabilization, and a practical product formulation that can be rehydrated reasonably quickly.

This and the earlier study using silkworm silk[3] demonstrate the ability of various silk proteins to significant stabilize viruses against thermal degradation. Use of these specific proteins for clinical applications such as for stabilization of vaccines will depend on how the body responds to the silk protein upon vaccine administration. Alternatively, peptides designed based on the composition of silk proteins may provide a route to utilize the stability conferred by the silk proteins but using a nonsilk protein. Applications involving use of agricultural viruses, such as for biocontrol agents, may consider silk protein formulations as an alternative to stabilize the viruses during transport and in the field.

■ CONCLUSIONS

This paper describes a simple method to directly measures viral infectivity that is suitable as a model system to assess stability of nonenveloped viruses under a range of environmental conditions. The assay was used to demonstrate that protein films stabilize viruses against elevated temperatures, and that silk proteins are superior to a model nonsilk protein, BSA. There is no obvious relationship between the amount of potentially ordered molecular structure in the protein films and ability to stabilize the virus. Furthermore, there was no obvious correlation between amount of β-sheets, the dominant molecular structure of silkworm silks, and the ability to stabilize the virus. Protein-induced modification of the hydration shell surrounding the virus coat proteins, and an increase in protein−protein interactions over water−protein interactions are likely mechanisms that stabilize the virus coat proteins and therefore underpin the stabilization of viral infectivity against exposure to elevated temperatures. These mechanisms are likely enhanced by the presence of proteins containing a high proportion of amino acids with small side chains and a flexible tertiary structure, possibly explaining why silk proteins were better able to protect viral infectivity over BSA.

■ ASSOCIATED CONTENT

ⓢ Supporting Information
Details of the amide I and amide III deconvolutions and TGA analysis for all of the films included in this study. This material is available free of charge via the Internet at http://pubs.acs.org.

■ AUTHOR INFORMATION

Corresponding Author
*T. D. Sutherland. E-mail: Tara.Sutherland@csiro.au.
Notes
The authors declare no competing financial interest.

■ ACKNOWLEDGMENTS

paper and Andrea Woodhead for assistance in collecting infrared spectra.

■ REFERENCES

(1) Harper, D. R. *Viruses: Biology, Application and Control*; Garland Science: New York, 2011.

(2) Cooke, B. D.; Fenner, F. Rabbit Haemorrhagic Disease and the Biological Control of Wild Rabbits, *Oryctolagus Cuniculus*, in Australia and New Zealand. *Wildlife Res.* **2002**, *29*, 689−706.

(3) Zhang, J.; Pritchard, E.; Hu, X.; Valentin, T.; Panilaitis, B.; Omenetto, F. G.; Kaplan, D. L. Stabilization of Vaccines and Antibiotics in Silk and Eliminating the Cold Chain. *Proc. Natl. Acad. Sci. U. S. A.* **2012**, *109*, 11981−11986.

(4) Chen, D.; Kristensen, D. Opportunities and Challenges of Developing Thermostable Vaccines. *Expert Rev. Vaccines* **2009**, *8*, 547−558.

(5) Pisal, S.; Wanwde, G.; Salvankar, S.; Lade, S.; Kadam, S. Vacuum Foam Drying for Preservation of Lasota Virus: Effect of Additives. *AAPS Pharm. Sci. Technol.* **2006**, *7*, E1−E5.

(6) Sutherland, T. D.; Young, J. H.; Weisman, S.; Hayashi, C. Y.; Merritt, D. J. Silk: One Name, Many Materials. *Annu. Rev. Entomol.* **2010**, *55*, 171−188.

(7) Saito, H.; Tabeta, R.; Asakura, T.; Iwanaga, Y.; Shoji, A.; Ozaki, T.; Ando, I. High-Resolution Carbon-13 NMR Study of Silk Fibroin in the Solid State by the Cross-Polarization-Magic Angle Spinning Method. Conformational Characterization of Silk I and Silk II Type Forms of *Bombyx Mori* Fibroin by the Conformation-Dependent Carbon-13 Chemical Shifts. *Macromolecules* **1984**, *17*, 1405−1412.

(8) Weisman, S.; Haritos, V. S.; Church, J. S.; Huson, M. G.; Mudie, S. T.; Rodgers, A. J. W.; Sutherland, T. D. Honeybee Silk: Recombinant Protein Production, Assembly and Fiber Spinning. *Biomaterials* **2010**, *31*, 2695−2700.

(9) Kameda, T.; Kojima, K.; Miyazawa, M.; Fujiwara, S. Z. Film Formation and Structural Characterization of Silk of the Hornet *Vespa Simillima Xanthoptera* Cameron. *Z. Naturforsch., C: J. Biosci.* **2005**, *60*, 906−914.

(10) Campbell, P. M.; Trueman, H. E.; Zhang, Q.; Koijima, K.; Kameda, T.; Sutherland, T.D. . Cross-Linking in the Silks of Bees, Ants and Hornets. *Insect Biochem. Mol. Biol.* **2014**, *48*, 40−50.

(11) Ciesek, S.; Friesland, M.; Steinmann, J.; Becker, B.; Wedemeyer, H.; Manns, M. P.; Steinmann, J.; Pietschmann, T.; Steinmann, E. How Stable is the Hepatitis C Virus (HCV)? Environmental Stability of HCV and its Susceptibility to Chemical Biocides. *J. Infect. Dis.* **2010**, *201*, 1859−1866.

(12) Abad, F. X.; Pinto, R. M.; Bosch, A. Survival of Enteric Viruses on Environmental Fomites. *Appl. Environ. Microb.* **1994**, *60*, 3704−3710.

(13) Peetermans, J. Factors Affecting the Stability of Viral Vaccines. *Dev. Biol. Stand.* **1996**, *87*, 97−101.

(14) Scherk, M. A.; Ford, R. B.; Gaskell, R. M.; Hartmann, K.; Hurley, K. F.; Lappin, M. R.; Levy, J. K.; Little, S. E.; Nordone, S. K.; Sparkes, A. H. 2013 AAFP Feline Vaccination Advisory Panel Report. *J. Feline Med. Surg.* **2013**, *15*, 785−808.

(15) Cleaveland, S.; Kaare, M.; Knobel, D.; Laurenson, M. K. Canine Vaccination—Providing Broader Benefits for Disease Control. *Vet. Microbiol.* **2006**, *117*, 43−50.

(16) Schultz, R. D. Duration of Immunity for Canine and Feline Vaccines: A Review. *Vet. Microbiol.* **2006**, *117*, 75−79.

(17) Yule, T. D.; Roth, M. B.; Dreier, K.; Johnson, A. F.; Palmer-Densmore, M.; Simmons, K.; Fanton, R. Canine Parvovirus Vaccine Elicits Protection from the Inflammatory and Clinical Consequences of the Disease. *Vaccine* **1997**, *15*, 720−729.

(18) Doel, T. R. FMD Vaccines. *Virus Res.* **2003**, *91*, 81−99.

(19) Rodriguez, L. L.; Grubman, M. J. Foot and Mouth Disease Virus Vaccines. *Vaccine* **2009**, *27*, D90−D94.

(20) Smid, B.; Valicek, L.; Rodak, L.; Stepanek, J.; Jurak, E. Rabbit Hemorrhagic-Disease - An Investigation of some Properties of the Virus and Evaluation of an Inactivated Vaccine. *Vet. Microbiol.* **1991**, *26*, 77−85.

(21) Koff, R. S. Hepatitis A. *Lancet* **1998**, *351*, 1643−1649.

(22) Stanley, M.; Lowy, D. R.; Frazer, I. Prophylactic HPV Vaccines: Underlying Mechanisms. *Vaccine* **2006**, *24*, 106−113.

(23) Soares-Weiser, K.; MacLehose, H.; Bergman, H.; Ben-Aharon, I.; Nagpal, S.; Goldberg, E.; Pitan, F.; Cunliffe, N. Vaccines for Preventing Rotavirus Diarrhoea: Vaccines in Use. *Cochrane Database Syst. Rev.* **2012**, *2*, CD008521.

(24) Polio Vaccines and Polio Immunization in the Pre-Eradication Era: WHO Position Paper. *Wkly. Epidemiol. Rec.* **2014**, *89*, 73−92.

(25) Lu, T. K; Koeris, M. S. The Next Generation of Bacteriophage Therapy. *Curr. Opin. Microbiol.* **2011**, *14*, 524−531.

(26) Gilmore, B. F. Bacteriophages as Anti-Infective Agents: Recent Developments and Regulatory Challenges. *Expert Rev. Anti. Infect. Ther.* **2012**, *10*, 533−535.

(27) Kameda, T. Influence of pH, Temperature and Concentration on Stabilization of Aqueous Hornet Silk Solution and Fabrication of Salt-Free Materials. *Biopolymers* **2014**, in press.

(28) Savitzky, A.; Golay, M. J. E. Smoothing and Differentiation of Data by Simplified Least Squares Procedures. *Anal. Chem.* **1964**, *36*, 1627−1639.

(29) Tretinnikov, O. N.; Tamada, Y. Influence of Casting Temperature on the Near-Surface Structure and Wettability of Cast Silk Fibroin Films. *Langmuir* **2001**, *17*, 7406−7413.

(30) Lawrence, B. D.; Omenetto, F.; Chui, K.; Kaplan, D. L. Processing Methods to Control Silk Fibroin Film Biomaterial Features. *J. Mater. Sci.* **2008**, *43*, 6967−6985.

(31) Reisdorf, W. C.; Krimm, S. Infrared Amide I' Band of the Coiled Coil. *Biochemistry* **1996**, *35*, 1383−86.

(32) Heimburg, T.; Schuenemann, J.; Weber, K.; Geisler, N. Specific Recognition of Coiled Coils by Infrared Spectroscopy: Analysis of the Three Structural Domains of Type III Intermediate Filament Proteins. *Biochemistry* **1996**, *35*, 1375−1382.

(33) Heimburg, T.; Schunemann, J.; Weber, K.; Geisler, N. FTIR-Spectroscopy of Multistranded Coiled Coil Proteins. *Biochemistry* **1999**, *38*, 12727−12734.

(34) Byler, D. M.; Susi, H. Application of Computerized Infrared and Raman Spectroscopy to Conformation Studies of Casein and other Food Proteins. *J. Ind. Microbiol.* **1988**, *3*, 73−88.

(35) Singh, B. R.; DeOliveira, D. B.; Fu, F.-N.; Fuller, M. P. Fourier Transform Infrared Analysis of Amide III Bands of Proteins for the Secondary Structure Estimation. In *Proceedings of Biomolecular Spectroscopy III*, Los Angeles, CA, January 17−18, 1993; Nafie, L. A., Mantsch, H. H., Eds.; Proceedings of SPIE Series, Vol. *1890*, 1993; doi: 10.1117/12.145242.

(36) Cai, S.; Singh, B. R. Identification of beta-Turn and Random Coil Amide III Infrared Bands for Secondary Structure Estimation of Proteins. *Biophys. Chem.* **1999**, *80*, 7−20.

(37) Sutherland, T. D.; Weisman, S.; Walker, A. A.; Mudie, S. T. The Coiled Coil Silk of Bees, Ants and Hornets. *Biopolymers* **2012**, *97*, 446−454.

(38) Sutherland, T. D.; Trueman, H. E.; Walker, A. A.; Weisman, S.; Campbell, P. M.; Dong, Z.; Huson, M. G.; Woodhead, A. L.; Church, J. S. Convergently-Evolved Structural Anomalies in the Coiled Coil Domains of Insect Silk Proteins. *J. Structural. Biol.* **2014**, *186*, 402−411.

(39) Fu, K.; Griebenow, K.; Hsieh, L.; Klibanov, A. M.; Robert, L. FTIR Characterization of the Secondary Structure of Proteins Encapsulated Within PLGA Microspheres. *J. Controlled Release* **1999**, *58*, 357−366.

(40) Fenimore, P. W.; Frauenfelder, H.; McMahon, B. H.; Young, R. D. Bulk-Solvent and Hydration-Shell Fluctuations, Similar to α- and β-Fluctuations in Glasses, Control Protein Motions and Functions. *Proc. Natl. Acad. Sci. U. S. A.* **2004**, *101*, 14408−14413.

(41) Danielewicz-ferchmin, I.; Banachowicz, E.; Ferchmin, A. R. Protein Hydration and the Huge Electrostriction. *Biophys. Chem.* **2003**, *106*, 147−153.

(42) Zhao, H. Viscosity *B*-Coefficients and Standard Partial Molar Volumes of Amino Acids, and their Roles in Interpreting the Protein (Enzyme) Stabilization. *Biophys. Chem.* **2006**, *122*, 157−183.

(43) Fernández, A.; Scheraga, H. A. Insufficiently Dehydrated Hydrogen Bonds as Determinants of Protein Interactions. *Proc. Natl. Acad. Sci. U. S. A.* **2003**, *100*, 113−118.

(44) Kamerzell, T. J.; Middaugh, C. R. The Complex Inter-Relationships Between Protein Flexibility and Stability. *J. Pharm. Sci.* **2008**, *97*, 3494−3517.

(45) Chi, E. Y.; Krishnan, S.; Randolph, T. W.; Carpenter, J. F. Physical Stability of Proteins in Aqueous Solutions: Mechanism and Driving Forces in Nonnative Protein Aggregation. *Pharm. Res.* **2003**, *20*, 1325−1336.

(46) Wolfenden, R.; Andersson, L.; Cullis, P. M.; Southgate, C. C. B. Affinities of Amino Acid Side Chains for Solvent Water. *Biochemistry* **1981**, *20*, 849−855.

18196

dx.doi.org/10.1021/am5051873 | *ACS Appl. Mater. Interfaces* 2014, 6, 18189−18196